A CNN ARCHITECTURE TAILORED FOR QUANTUM FEATURE MAP-BASED RADAR SOUNDER SIGNAL SEGMENTATION

Raktim Ghosh^{1,2}, Amer Delilbasic^{3,4,5}, Gabriele Cavallaro^{3,4}, Francesca Bovolo²

¹ University of Trento, Italy, and ² Fondazione Bruno Kessler, Trento, Italy
³ Jülich Supercomputing Centre, Forschungszentrum Jülich, Germany
⁴ School of Engineering and Natural Sciences, University of Iceland, Iceland
⁵ Φ-lab, ESRIN, European Space Agency, Italy

ABSTRACT

This article presents a hybrid quantum-classical framework by incorporating quantum feature maps regulated classical Convolutional Neural Network (CNN) architecture in the context of detecting different subsurface targets in the radar sounder signal. The quantum feature maps are generated by quantum circuits to utilize spatially-bound input information from the input training samples. The associated spectral probabilistic amplitudes of the feature maps are further fed as an input to the classical CNN-based network to classify the subsurface targets in the radargram. Experimental results on the MCoRDS and MCoRDS3 dataset demonstrated the capability of contextualizing the classical architecture through quantum feature maps for characterizing the radar sounder data.

Index Terms— radar sounder, quantum computing, quantum machine learning, subsurface sensing, segmentation

1. INTRODUCTION

Radar Sounders are spaceborne or airborne nadir looking sensors with active sensing capabilities that transmit linearly modulated Electromagnetic (EM) pulses and receive backscattered echoes from the subsurface targets depending upon the geometric properties of the targets, dielectric discontinuities, etc. These sensors operate on the range of High Frequency (HF) to Very High Frequency (VHF) bands [1]. After the backscattered echoes are collected, a coherent integration of these echoes is performed by compression techniques (range and azimuth) with Synthetic Aperture Radar (SAR) Focusing to generate radargram [2]. A number of post-processing tasks (such as clutter suppression, platform instability corrections) are also taken into account in the overall pipeline for generating the final high-level product. These radargrams are utilized for miscellaneous tasks such as estimating geophysical properties, subsurface target identification, semantic segmentation,

etc. A significant research activities have been carried out over the last few years to characterize the radargrams by incorporating miscellaneous supervised and unsupervised segmentation techniques by utilizing Convolutional Neural Network (CNN) based architectures or Transformers networks [3, 4].

Over the last few years, Quantum Machine Learning (QML) has been proliferated as a rapidly emerging and evolving field with a view to improving the overall framework of classical machine learning problems. OML is broadly associated to the principle of quantum mechanics applied to quantum computing tasks to perform measurement by Quantum Computers. [5] proposed a combinatorial framework with 4 different categorizations of QML-i) Classical-Classical (CC), ii) Classical-Quantum (CQ), iii) Quantum-Classical (QC), and iv) Quantum-Quantum (QQ). While CC approaches are fully classical agent interacting with classical environment, CQ settings may investigate how classical learning framework interact in aiding quantum tasks. QC approaches are the quantum-inspired learning framework with classical environmental settings. While considering OML, OC approaches investigate the potential enhancement of classical environment with quantum devices. More generally, the Hybrid OC (HOC) architecture may exploit imperfect Noisy Intermediate-Scale Quantum (NISQ) devices for selected computations on quantum hardware. Lastly, the QQ approaches fully exploit the quantum infrastructure for carrying out OML on quantum data [6]. A number of quantum algorithms are developed in various domains ranging from search optimization, quantum cryptography, quantum simulations in physics-based problems, etc [7]. In the domain of remote sensing image classification, [8] developed a gate-based quantum computing with a HQC architecture for classifying remote sensing images, [9] incorporated Quantum SVM algorithm on a quantum annealing framework for classifying remote sensing images. Recently, [10] developed a HQC architecture for multispectral remote sensing image classification problems by utilizing the features extracted from quantum circuits. While considering the domain of radar sounder, so far there is no attempt to utilize quantum feature maps for classifying the subsurface

This work was supported by the Italian Space Agency through the "Missione JUICE - Attività dei team scientifici dei Payload per Lancio, commissioning, operazioni e analisi dati" Agenzia Spaziale Italian-Istituto Nazionale di Astrofisica (ASI-INAF), under Contract 2023-6-HH.0.

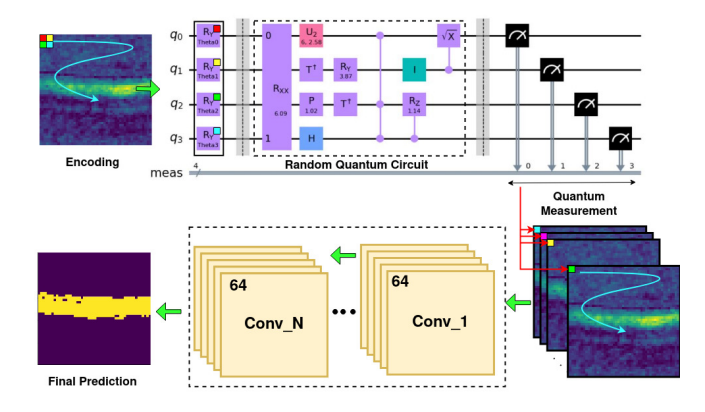


Fig. 1. A Schematic Layout of CNN Architecture tailored with Quantum Feature Maps generated through a 4-qubit random quantum circuit.

targets in radargrams.

This study aims to explore the potential of QC in the context of radar sounder signal segmentation. Our work is adopted from the framework of [11]. However, we utilize a Bellman quantum circuit [8] as well as a Random quantum circuit [11] to generate quantum feature maps and assess the performance on the classical CNN architecture. Experimental results demonstrated that the quantum feature maps derived from the quantum circuits depict a rich spectral probabilistic information for the overall learning framework in the context of radar sounder signal.

2. PROPOSED METHODOLOGY

Let us denote a radargram patch as a 2-D matrix R:

$$R = \{R(i,j)|i \in X = [1,...,n_T], j \in Y = [1,...,n_S]\}$$
 (1)

where $[1, ..., n_T]$ is the number of traces in the azimuth direction, and $[1, ..., n_S]$ is the number of samples along the range direction.

We denote N as the number of training patches as $\{(X_1, X_2, ..., X_N)\}$ and associated labels as $\{(L_1, L_2, ..., L_N)\}$ with the spatial dimension of X_i is [H, W] ($i \in 1, 2, ..., N$). The proposed method aims at classifying each pixel of radargrams into c distinct classes.

Figure 1 shows the overall schematic layout of the segmentation architecture for the radar sounder data. At first, the classical information from the input training patches is injected into the parameterized quantum circuits to measure the probability amplitudes with respect to the states of different qubits. Here, probability amplitudes refer to corresponding probabilities of collapsing of the qubits with the possible basis states. These probability amplitudes generate the quantum feature maps with the dimension corresponding to 2^d for a d-qubit quantum system. After that, the quantum feature

maps flow through convolutions to measure the probabilities for final class-wise predictions.

successive convolution operations are performed on these quantum feature maps to measure the probabilities for final class-wise predictions.

2.1. Quantum Feature Maps

We extract spatially-bound local information by square filtering each X_i with a filter of size $q \times q$. For q =2, let us denote such neighbourhood with size 2×2 as $[\alpha_{m,n}, \alpha_{m+1,n}, \alpha_{m,n+1}, \alpha_{m+1,n+1}]$ $(m \in \{1, 2, ..., H\})$ and $n \in \{1, 2, ..., W\}$). The size of the filter corresponds to the number of qubits in the quantum circuits. For each qubit, rotation operators (θ_k) are utilized to project the qubits into the Hilbert space. The parameters θ_k in the rotation operators are injected with the localized classical information $[\alpha_{m,n}, \alpha_{m+1,n}, \alpha_{m,n+1}, \alpha_{m+1,n+1}]$. Therefore, for each spatial location of $q \times q$, a $2^{q \times q}$ dimensional vector is created by taking the probability amplitudes associated to the corresponding states estimated through quantum circuits. The successive convolution operations with the spatial dimension of the filter $q \times q$ across the image domain [H, W] will produce $2^{q \times q}$ feature maps each with size [H, W]. The spatial dimension of the final tensors of the quantum feature maps is $[2^{q \times q}, H, W]$. These probabilistic spectral information embedded into the quantum feature maps is utilized in the successive CNN layers for the tasks of semantic segmentation.

2.2. Quantum Circuits

In this work, we utilize a standard quantum circuit from the IBM Qiskit framework, and a random quantum circuit as a quantum feature map generator.

2.2.1. Bellman Quantum Circuit

The first circuit is the Bellman Quantum Circuit which is utilized as a Quantum feature map generator. By utilizing a Hadamard gate on a first qubit, and successive CNOT gates between the consecutive qubits, the circuit prepares an entangled state at the first place. After establishing quantum correlations through Entanglement, the qubits are rotated along the *y*-axis with parameters θ_k . These θ_k values are the spatially bound classical information $[\alpha_{m,n},\alpha_{m+1,n},\alpha_{m,n+1},\alpha_{m+1,n+1}]$ for a 4-qubit system convolved with a 2×2 filter across dimension [H,W] for a training sample X_i . After the operation of rotated entangled state of the system, the CNOT processes are mirrored with respect to preceding CNOT operations before the rotations of qubits through *y*-axis.

2.2.2. Random Quantum Circuit

Figure 3 depicts a random quantum circuit. At first, the encoding is performed by injecting the classical values (from

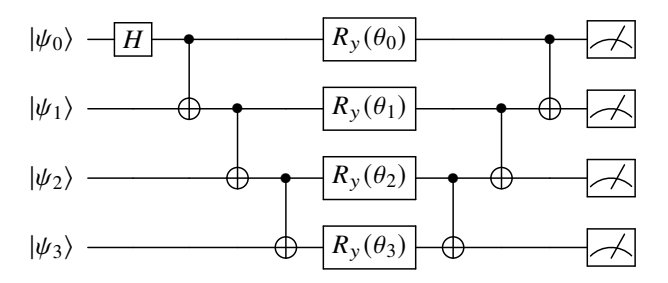


Fig. 2. A Schematic Layout of Bellman Quantum Circuit adopted from [8]

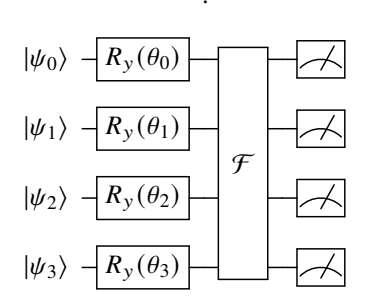


Fig. 3. A Schematic Layout of Random Quantum Circuit

input training samples) into the rotation gates for each qubits. Subsequently, several arbitrary unitary operators comprising different quantum gates are incorporated, depending on the user-defined depth of the quantum system. Lastly, the measurement is done on the random quantum circuits and the corresponding probability amplitudes are utilized as inputs to the classical neural networks.

2.3. CNN Layers

We denoted the tensor dimension of the generated quantum feature maps are $[2^{q\times q}, H, W]$. The dimension of the quantum feature tensors $[2^{q\times q}, H, W]$ are raised to K, where K is greater than $2^{q\times q}$. After utilizing CNN layers during training, the dimension of the tensor is reduced to the number of classes. Therefore, the final tensor dimension is [c, H, W].

3. EXPERIMENTAL RESULTS

3.1. Dataset

We tested our proposed architecture on the MCoRDS and MCoRDS3 dataset hosted by CReSIS unit. The operating bandwidth of these sensors are 9.5 MHz and 30 MHz. The operational aircraft height was about 7000 m for the MCoRDS dataset. On the other hand, the aircraft altitude is about 500 m. The campaign took place over the Antarctica ranging from $(-86^{\circ}00'\text{N to} -15^{\circ}67'\text{E})$ to $(-86^{\circ}02'\text{N to} 29^{\circ}45'\text{E})$ dated on November 2010. While considering the MCoRDS dataset, a total 27350 number of traces are considered covering 400 line-km with 8 radargrams. In case of MCoRDS3 dataset,

a total 30009 number of range lines are considered and the campaign took place in the Greenland (inland) on 2017.

3.2. Experimental Setup

The radargrams are labelled manually along the azimuth and range directions with respect to the distinct subsurface labels. We extracted consecutive non-overlapping spatial patches along the azimuth directions for the MCoRDS and MCoRDS3 dataset. Here, we design a simple binary segmentation problem by focusing on the deepest radargram portion where can find only the noise and the bedrock. This reduces the computational burden of generating quantum feature maps from input training samples. However, more classes can be considered. By identifying the bedrock through labels, the patches are extracted across the thickness of bedrock in the range directions. The spatial dimensions of each training sample are kept as 50×50 during training and testing. 800 samples are utilized for training and 254 samples are kept for testing. To derive the quantum feature maps, a spatial filter $w \times w = 2 \times 2$ is utilized to extract 4 classical values (denoted previous in Section 2 as $[\alpha_{m,n}, \alpha_{m+1,n}, \alpha_{m,n+1}, \alpha_{m+1,n+1}]$ in successive convolutional step. These 4 classical values are injected into the rotation gates (along the y-axis) of a 4 – qubit qubit quantum system. To measure the probability amplitudes for every joint 4 - qubit basis states, 512 shots are utilized with IBM AerSimulator as a backend simulator. In case of successive CNN operations on the derived quantum feature maps, a CNN network with kernel size with 3×3 and 64 number of filters are utilized to raise the dimension of the tensors from the quantum feature maps from 16 to 64. The probability amplitudes together with the associated labels are used for training the CNN architecture. For the final predictions, we reduce the channel dimension according to the corresponding classes. We utilize the training iterations as 100 with a constant learning rate of 1e - 5. The batch size is kept as 16. For assessing the overall performance of the proposed network, we utilize F1-score and Overall Accuracy (OA) as evaluation metrics.

3.3. Segmentation Results

In Table 1, we report the quantitative results of the proposed CNN architecture associated with the Bellman Quantum, and Random Quantum Circuit along with the classical counterpart of the CNN architecture. We carried out an ablation of the CNN layers varying from 1 to 4 with 64 number of filters in each layer. In classical counterpart, the quantum feature maps are not utilized while training the CNN architecture. Quantitatively, the performance of the HQC architecture and the classical counterpart is similar. However, we observed a slight gain of accuracy (against classical counterpart) while considering a one-layered CNN architecture tailored with quantum feature maps. According to our observation, the entanglement in Bellman circuit played a crucial role in transforming the input

CNN Layers	L-1		L-2		L-3		L-3	
Algorithms	F1-Score	OA	F1-Score	OA	F1-Score	OA	F1-Score	OA
HQC (Bellman Circuit)	0.6713	86.35	0.7028	87.93	0.7373	89.22	0.7565	89.99
HQC (Random Circuit)	0.6700	86.39	0.7081	88.04	0.7214	88.82	0.7553	90.00
Classical Counterpart	0.6526	85.79	0.7084	87.89	0.7366	89.21	0.7537	89.96

information into a quantum framework thereby demonstrating the potential of quantum mechanical phenomena as a rich feature descriptor. Further, it is noteworthy that the spectral probabilistic information generated through these two quantum circuits achieved similar set of accuracy with the classical counterpart. Therefore, the quantum feature maps generated through the miscellaneous quantum circuits turned out to be rich spectral information.

4. CONCLUSIONS

In this work, we explored the potential of quantum feature map regulated CNN architecture for semantic segmentation of the radar sounder data. Due to lack of current hardware infrastructure to generate quantum feature maps with computational complexity, the spatial dimension of the training patches are restricted to 50×50 . In future work, we will explore the quantum feature maps regulated generative models to exploit the generalizability of the quantum features for radar sounder signal.

5. REFERENCES

- [1] Leonardo Carrer, Christopher Gerekos, Francesca Bovolo, and Lorenzo Bruzzone, "Distributed radar sounder: A novel concept for subsurface investigations using sensors in formation flight," *IEEE Transactions on Geoscience and Remote Sensing*, vol. 57, no. 12, pp. 9791–9809, 2019.
- [2] A. Ilisei and L. Bruzzone, "A system for the automatic classification of ice sheet subsurface targets in radar sounder data," *IEEE TGRS*, vol. 53, pp. 3260–3277, 2015.
- [3] R. Ghosh and F. Bovolo, "Transsounder: A hybrid transunet-transfuse architectural framework for semantic segmentation of radar sounder data," *IEEE TGRS*, vol. 60, pp. 1–13, 2022.
- [4] R. Ghosh and F. Bovolo, "An enhanced unsupervised feature learning framework for radar sounder signal segmentation," in *IGARSS* 2023 2023 IEEE IGARSS, 2023, pp. 6920–6923.

- [5] Vedran Dunjko, Jacob M. Taylor, and Hans J. Briegel, "Quantum-enhanced machine learning," *Physical review letters*, vol. 117 13, pp. 130501, 2016.
- [6] Lirandë Pira and Chris Ferrie, "An invitation to distributed quantum neural networks," *Quantum Mach. Intell.*, vol. 5, no. 2, Dec. 2023.
- [7] J. Biamonte, P. Wittek, N. Pancotti, P. Rebentrost, N. Wiebe, and S. Lloyd, "Quantum machine learning," *Nature*, vol. 549, no. 7671, pp. 195–202, Sept. 2017.
- [8] A. Sebastianelli, D. Zaidenberg, D. Spiller, B. Saux, and S. Ullo, "On circuit-based hybrid quantum neural networks for remote sensing imagery classification," *IEEE JSTARS*, vol. 15, pp. 565–580, 2022.
- [9] A. Delilbasic, G. Cavallaro, M. Willsch, F. Melgani, M. Riedel, and K. Michielsen, "Quantum support vector machine algorithms for remote sensing data classification," in 2021 IEEE International Geoscience and Remote Sensing Symposium IGARSS, 2021, pp. 2608– 2611.
- [10] F. Fan, Y. Shi, and X. X. Zhu, "Urban land cover classification from sentinel-2 images with quantum-classical network," in *2023 JURSE*, 2023, pp. 1–4.
- [11] Maxwell Henderson, Samriddhi Shakya, Shashindra Pradhan, and Tristan Cook, "Quanvolutional neural networks: Powering image recognition with quantum circuits," 2019.